Small Panchromatic and NIR Absorbers from Quinoid Zwitterions

Angélina Torres Ruiz, Manon Bousquet, Simon Pascal, Gabriel Canard, Valérie Mazan, Mourad Elhabiri, Denis Jacquemin, Olivier Siri

Small Panchromatic and NIR Absorbers from Quinoid Zwitterions

Angélina Torres Ruiz,[a] Manon H. E. Bousquet,[b] Simon Pascal,*[,a] Gabriel Canard,[a] Valérie Mazan,[c] Mourad Elhabiri,[c] Denis Jacquemin,*[,b] Olivier Siri*[,a]

[a] *Aix-Marseille Univ, CNRS UMR 7325, Centre Interdisciplinaire de Nanoscience de Marseille (CINaM), Campus de Luminy, 13288 Marseille cedex 09, France.*

[b] *Laboratoire CEISAM, CNRS UMR 6230, Université de Nantes, 2, rue de la Houssinière, 44322 Nantes, France.*

[c] *Université de Strasbourg, Université de Haute-Alsace, CNRS, LIMA, UMR 7042, Equipe Chimie Bioorganique et Médicinale, ECPM, 25 Rue Becquerel, 67000 Strasbourg, France.*

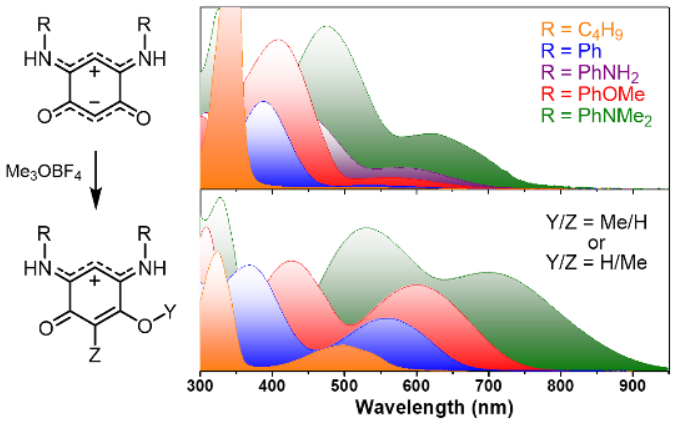

ABSTRACT

The transamination of oxoaminobenzoquinonemonoimine (BQI derivatives), an unconventional zwitterionic quinone, allows isolating a series of compounds featuring electron-donating aryl auxochromes. The substitution has a very strong impact on the electrochemical and optical features, which is rationalized by theoretical calculations. Protonation and alkylation of the BQIs towards the corresponding cations lead to surprising redshifts of the absorption, especially in the instance of the most electron-rich dyes which exhibit panchromatic absorption spanning up to the near-infrared (NIR) region, a remarkable achievement for such small molecules.

Ground-state π-zwitterions are intriguing conjugated molecules featuring unique photophysical properties. In this family of dyes, the most simple representatives are the monocyclic 2,5-oxoamino-1,4-benzoquinonemonoimines (**Z** form of BQIs, Figure 1), featuring a stable zwitterionic ground state, that were reported for the first time in 2002.[1] The charge separation in BQI is due to an intramolecular proton transfer that generates two distinct 6π electrons subunits, *i.e.*, a positively charged trimethine cyanine and a negatively charged trimethine oxonol, linked through two single bonds (see **Z**-BQI, Figure 1). According to the coupling principle of polymethine dyes,[2] such ground state electronic structure is highly stable, which partly explains why the canonical isomer (**Q**-BQI) has never been isolated so far. Another proof of the high stability of **Z**-BQIs is that they were recently reported as natural products present in the marine sponge *Dactylospongia metachromia*,[3] which consists in a rare example of a *C*-substituted BQI.[4] During the last decade, the efficient *N*-substitution of BQIs with alkyl moieties *via* transamination reaction[5] paved the way to the use of this class of compounds as ditopic *bis*-bidentate ligands to design coordination complexes featuring original redox,[6] catalytic,[7] and vapochromic properties.[8] In parallel, the convenient functionalization of BQIs combined with their large intrinsic dipole (*ca.* 10 D) made them candidates of choice for the elaboration of molecular films following adsorption[9] or polymerization[10] on metallic surfaces along with interfaces,[11] and more recently as interlayer in graphene transistors.[12]

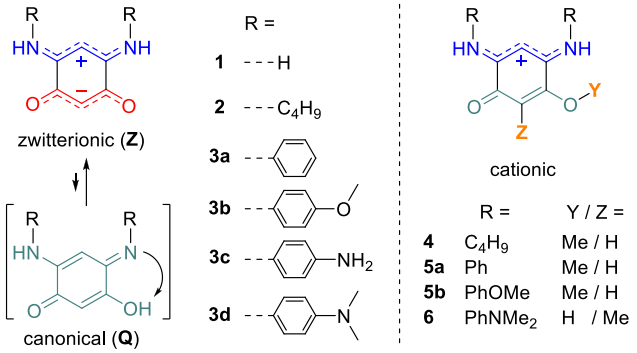

Figure 1. Canonical-zwitterionic equilibrium in BQI and scope of the zwitterionic and cationic derivatives synthesized.

However, aryl-substituted BQIs remain extremely scarce in the literature,[5b, 13] and, more generally, the redox and optical properties of the functionalized BQI zwitterions have been overlooked so far, as compared to the related azaacene[14] or quinonediimine-based zwitterionic analogues.[15] This remains surprising since BQIs are particularly small chromophores exhibiting absorption in the visible, as illustrated with unsubstituted BQI **1**, featuring a molecular weight of 138 Da and a purple coloration due to a broad though weak absorption between 450 and 650 nm (ε^{520} = 320 M^{-1} cm^{-1}). This work was undertaken to extend the scope of functionalized BQIs and highlight that *N*-substitution with electron-donating aryl moieties is a straightforward strategy to control their redox and optical properties. Herein, aryl-substituted BQIs were synthesized and the strong effect of the auxochromes was investigated using cyclic voltammetry and electronic absorption spectrophotometry that could be rationalized with *ab initio* approaches. Protonation, *O*- or *C*-alkylation reactions of these zwitterions lead to the identification of unprecedented panchromatic and near-infrared (NIR) absorbing cations, highlighting the considerable influence of the N-substituents (aryl *vs.* alkyl) on the optical properties.

The synthetic pathways to *N*-substituted BQIs rely on the reported transamination of compound **1** with an excess of amine (Scheme 1).[5b] The aryl substituents are intentionally selected as electron-rich since the transamination remains impossible with electron-poor anilines. Thanks to that strategy, BQIs **3a-d** were isolated as green to black solids after purification by simple precipitation. Compounds **2** and **3a,b** are efficiently *O*-alkylated using trimethyloxonium tetrafluoroborate to afford the corresponding cationic dyes **4** and **5a,b** with 50-73% yields. The regioselectivity of the methylation can be undoubtedly attributed by ^{1}H and ^{13}C NMR spectra which clearly show a molecular desymmetrization. Surprisingly, when a similar protocol was carried out using compound **3d**, the methylation occurred on the central carbon atom within the anionic subunit to afford the quinone **6** in only 17% yield, due to the large amount of remaining starting material. The structure of **6** was clearly evidenced by ^{1}H and ^{13}C NMR showing the absence of CH signal on the keto-enol subunit (see Figures S10-S12). Noteworthy, functionalization of BQIs at this position has only been observed in presence of cyano-derivatives (tetracyanoethylene, tetracyanoquinodimethane or dicyanobenzoquinone).[4] In the instance of **3d**, such reactivity is possible because of the symmetrical delocalization of the anionic charge within the 6π-electrons subunit.[16]

Scheme 1. Synthesis of zwitterionic and cationic BQIs.

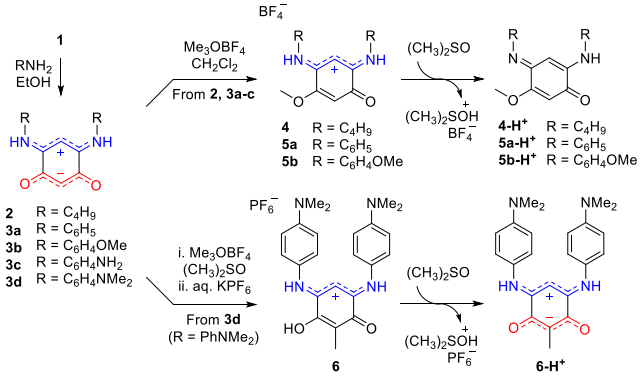

The cyclic voltammograms of the dyes were recorded in DCM solutions containing 0.1 M of [nBu$_4$NPF$_6$]. As a reference, *N*-alkyl zwitterion **2** presents a reversible reduction at -1.51 V *vs*. Fc/Fc$^+$ and an irreversible oxidation occurring at 0.83 V (Figure 2 and Table 1).[4a] Upon *N*-substitution with phenyl rings in **3a**, the reduction process is sensibly facilitated (-1.09 V) but becomes irreversible. As expected, the introduction of electron-donating groups on the aryl substituents shifts the reduction to lower voltages, with half-wave potentials found at -1.23, -1.27 and -1.31 V for compounds **3b**, **3c**, and **3d**, respectively. This trend is however accompanied by a lowering of the electrochemical gap (ΔE) due to the strong cathodic shifts of oxidations recorded for this series, with values varying from 0.71 to 0.19 V going from **3b** to **3d**, the latter exhibiting a reversible process. Upon *O*-alkylation, the reductions are noticeably facilitated in **4** and **5a,b**, with reversible processes found between -0.68 to -0.36 V, and a second reduction wave appears at *ca.* 1.40 V (see Figure S30). For these three cations, the oxidations are more arduous and found beyond 1.00 V. Finally, compound **6** features the lowest electrochemical gap of the series (0.99 V), with two reductions processes at -0.73 and -1.09 V, and an oxidation half-wave at 0.26 V.

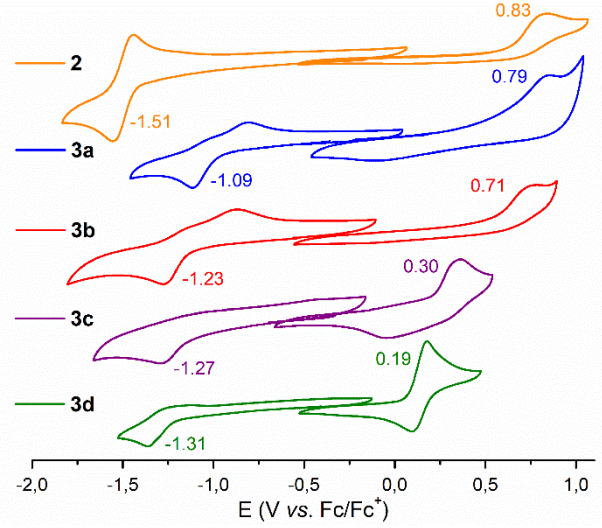

Figure 2. Cyclic voltammograms of compound **2** and **3a-d** in DCM containing 0.1 M of [nBu$_4$NPF$_6$].

The UV-vis-NIR absorption spectra recorded in DCM show that, in the case of *N*-alkyl-substituted **2**, the lower energy transition is found in the green region, at *ca*. 500 nm, and is characterized by a particularly low molar extinction coefficient of 200 M^{-1} cm^{-1} (Figure 3). This band is redshifted to 545 nm upon substitution with phenyl rings (**3a**) and its intensity is doubled to 440 M^{-1} cm^{-1}.

Table 1. Electrochemical[a] and optical properties in DCM solution.

Dye	$E_{1/2}$ red2	$E_{1/2}$ red1	$E_{1/2}$ ox1	ΔE	λ_{max} (nm)	ε (M^{-1} cm^{-1})
2	-	–1.51 (1.1)[b]	0.83	2.34	503	200
3a	-	–1.09	0.79	1.88	545	440
3b	-	–1.23	0.71	1.94	563	1300
3c	-	–1.27	0.30	1.57	576	2400
3d	-	–1.31	0.19 (1.0)[b]	1.50	623	6100
4	–1.37 (1.3)[c]	–0.68 (1.1)[b]	1.03	1.71	497	2250
5a	–1.41	–0.36 (1.3)[c]	1.01	1.37	554	4700
5b	–1.46	–0.46 (1.3)[b]	1.06	1.52	599	7600
6	–1.09	–0.73	0.26	0.99	697	8700

[a] Half-wave potential (V *vs*. Fc/Fc$^+$) of the compounds recorded in DCM solutions containing 0.1 M of [nBu$_4$NPF$_6$] (Pt electrode, scan rate: 100 mV s^{-1}). [b] Reversible and [c] pseudo-reversible processes with the corresponding peak current ratio i_{pc}/i_{pa} indicated in parentheses.

Interestingly, substitution with electron-rich aryls achieves important bathochromic and hyperchromic shifts of the lower energy transition towards the orange-red region, with absorption maxima centered at 563, 576, and 623 nm for **3b**, **3c**, and **3d**, respectively, and with a molar extinction coefficient reaching 6100 M^{-1} cm^{-1} for **3d**. Both the position and intensity of the second peak are impacted by the aryl substitution: while it is originally centered *ca*. 350 nm for **2** (ε^{350} ~ 30,000 M^{-1} cm^{-1}), this band is found to lie at 387 nm for compound **3a** and undergoes a strong hypochromic effect (ε^{387} ~ 9,700 M^{-1} cm^{-1}). For **3d**, featuring the strongest electron-donating substituents, the second transition is redshifted to the visible region, at 475 nm. The absorption solvatochromism recorded for compounds **1**, **2**, and **3a** shows a slight hypsochromic shift of the lower energy transition (Figure S32). Almost no change is found for both **3b** and **3c** and a bathochromic shift is noticed for **3d**, for which a charge transfer character is obtained by theory (see below).

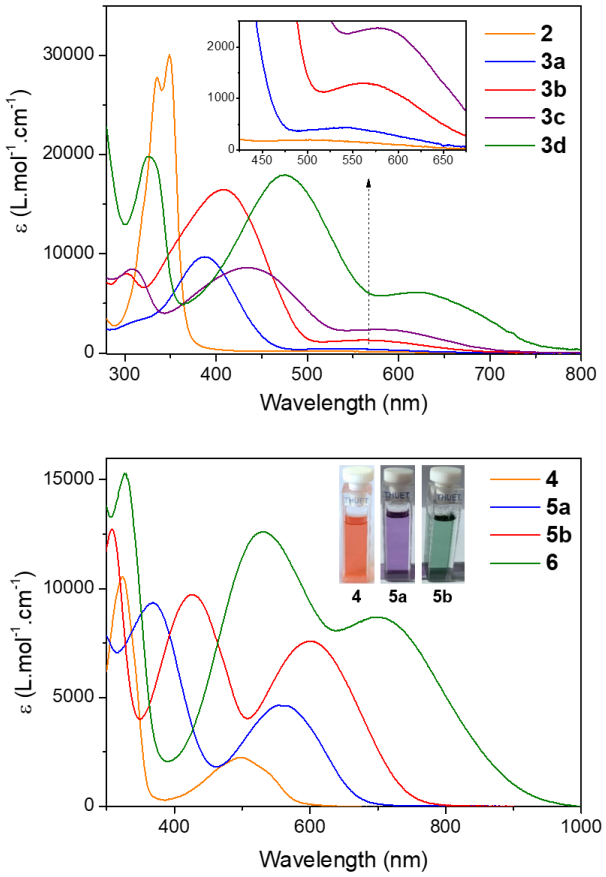

Figure 3. Electronic absorption spectra of zwitterions **2** and **3a-d** (top), and cations **4**, **5a,b** and **6** (bottom) in DCM.

To gain further insights into the properties of the aryl-substituted BQIs, the absorption properties were recorded under basic or acidic conditions (Figure S33 and S34). In presence of 1,8-diazabicyclo[5.4.0]undec-7-ene (DBU), both visible and UV transitions of compounds **3a-d** are significantly blue-shifted, which is explained by the deprotonation of the cationic subunit of the BQIs (*e.g.* **3d-H$^+$** in Scheme 2), resulting in a quenching of the intramolecular charge transfer (CT). In contrast, in presence of trifluoroacetic acid (TFA), the maximum of absorption gains in intensity and is surprisingly redshifted, with for instance λ_{max} centered at 694 nm in the case of compound **3d**, and with a cut-off value reaching 950 nm. The absorption pH-dependence of BQIs **3a** and **3d** were investigated in a mixture of MeOH/H_2O (8:2, w/w) (Figure S35 and S36). While the redshift of absorption of **3a** is unambiguously attributed to the protonation of the anionic subunit (pK_a = 8.64 ± 0.05), three species were identified upon two successive protonation steps of **3d** (Scheme 2). In fact, the first protonation occurs on the anionic oxonol and is responsible for the strong redshift in absorption (pK_a = 10.49 ± 0.04). The second protonation occurs on a tertiary N-atom of the aryl substituent (pK_a = 2.99 ± 0.06) and causes a moderate decrease of the molar extinction coefficient due to a partial quenching of the CT.

Scheme 2. Chemical structures generated upon (de)protonation of zwitterionic 3d.

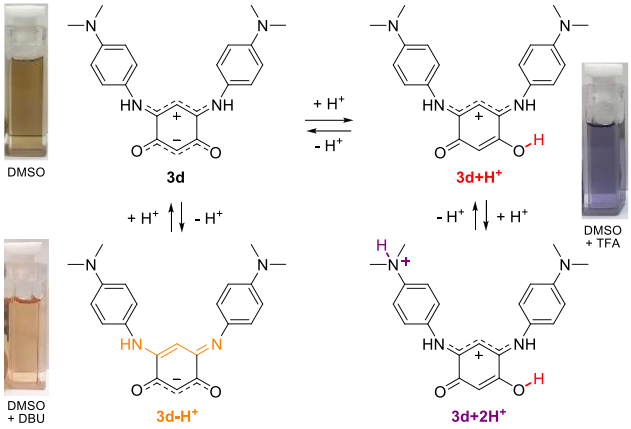

The effect of oxonol subunit protonation is mimicked by *O*-alkylation in cations **4**, **5a,b** and, consequently, their absorption is strongly redshifted in the visible range (Figure 3). While cation **4** presents a moderately intense absorption *ca.* 500 nm, compound **5a** shows hyper- and bathochromic shifts. Cation **5b**, with an absorption maximum at 599 nm, exhibits panchromatic absorption. Eventually, compound **6** also shows a maximum at 697 nm, the spectrum spanning over the whole visible range with a cut-off value reaching the NIR *ca.* 950 nm. Surprisingly, this series of alkylated BQIs (**4**, **5a,b**) shows an unexpected solvatochromic behavior. As an example, while compound **5a** is cationic in DCM solution (λ_{max} = 564 nm), a noticeable blueshift is monitored in DMSO, with λ_{max} = 502 nm (Figure S34), and is attributed to the solvent-mediated deprotonation towards the uncharged quinoidal species **5a-H$^+$** (Scheme 1).[17] In the case of **6**, deprotonation to zwitterionic **6-H$^+$** occurs in DMSO and shifts the absorption maximum to 481 nm. Such deprotonation in polar solvents observed for **6** is not recorded in the cases of other zwitterions **2** and **3a-d** (Figure S33) and is presumably due to the presence of the central methyl substituent on **6** that destabilizes the anionic charge of the oxonol subunit.

We have performed theoretical calculations *(i)* to characterize the **Z**/**Q** tautomeric equilibrium of all dyes and *(ii)* to rationalize their optical signatures. For all compounds, theory predicts that there is a strong dominance (97-100%) of zwitterionic forms in solution: the **Z** form is more stable by *ca.* 2 to 6 kcal.mol^{-1} as compared to the **Q** structure (Table S8). The lowest energy transition in **1** is computed at 544 nm with a very low oscillator strength (*f*=0.005, Table S9) in good match with the experimental evidences (Figure 3). This transition corresponds to pure HOMO-LUMO (H-L) transition accompanied by a significant CT from the negatively charged cyanine towards the positively charged cyanine (see Figure 4 and S38). This CT is accompanied by a decrease of the dipole moment (-3.1 D, see Table S7) consistent with a decrease of the zwitterionic character after absorption. When moving to **3a**, the lowest transition shows a doubled oscillator

strength, consistent with the experiment. This transition is still dominated by a H-L excitation and essentially presents the same CT character characterized by a drop of the dipole moment by -3.8 D. In **3c**, the transition predicted at 582 nm becomes more intense (*f*=0.091). It conserves a dominant, yet not pure H-L character (Table S9). This time the change of polarity is trifling (dipole decrease of -0.4 D only), and the transition essentially corresponds to a quadrupolar CT from the top and bottom cyanines towards the C–C single bonds (Figure S46). Eventually, for **3d**, the transition is further redshifted to 606 nm (*f*=0.211), consistent with experiment. The transition shows a mixed MO composition, but the H-L transition now corresponds to a CT from the aniline towards the core of the BQI, with an increase of dipole moment of 3.0 D, consistent with the observed positive solvatochromism (Figure 4). Noteworthy, theory shows that, in contrast to larger aza-acenes,[14] the dihedral angles between the core and the *N*-substituted phenyls decreases together with the absorption energy, depending on the donor strength (see Figures S40-S42). Finally, the spectral features of the cationic species **4**, **5a** and **5b** were calculated, showing maxima relevant with the experimental data (Figures S48-S50).

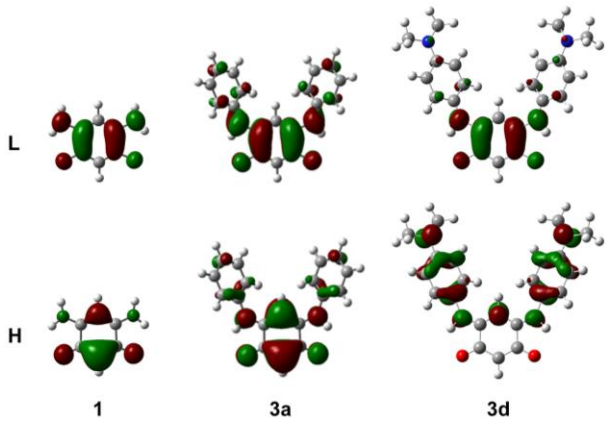

Figure 4. Representation of the frontier MOs for **1**, **3a**, and **3d**. H: HOMO; L: LUMO.

In brief, we synthesized and investigated the optical and physico-chemical properties of small zwitterionic and cationic BQIs, including an unprecedented *C*-alkylated cation **6**. We clearly demonstrated the drastic effect of the *N*-aryl substituents, highlighting unique properties in quinoid chemistry. Compounds **2** and **3a-d** revealed tunable oxidation processes and absorption maxima depending on the nature of the *N*-substitution. Cationic BQIs **5b** and **6**, synthesized in only two steps and with molecular weights lower than 400 Da, show high solubility and panchromatic absorptions spanning to the NIR range that are relevant for organic photovoltaic and photodetector applications.

ASSOCIATED CONTENT

Supporting Information

The Supporting Information is available free of charge on the ACS Publications website:
https://pubs.acs.org/doi/10.1021/acs.orglett.0c02926
Experimental, computational, and spectroscopic characterization data are included (PDF)
Crystallographic file for compound **2** can be found at CCDC 2027729.

AUTHOR INFORMATION

Corresponding Authors

*E-mail: pascal@cinam.univ-mrs.fr
*E-mail: Denis.Jacquemin@univ-nantes.fr
*E-mail: olivier.siri@univ-amu.fr

Author Contributions

‡ These authors contributed equally.

Notes

The authors declare no competing financial interest to this work.

ACKNOWLEDGMENT

We thank the *Région SUD* for the attribution of a PhD grant to ATR. This work used the computational resources of the CCIPL center installed in Nantes thanks to the support of the *Région des Pays de la Loire*. We are thankful to the *Spectropole* (*Fédération Sciences Chimiques Marseille*) for XRD analysis.

REFERENCES

(1) (a) Siri, O.; Braunstein, P., *Chem. Commun.* **2002**, 208; (b) Braunstein, P.; Siri, O.; Taquet, J.-p.; Rohmer, M.-M.; Bénard, M.; Welter, R., *J. Am. Chem. Soc.* **2003,** *125*, 12246.
(2) Dähne, S.; Leupold, D., *Angew. Chem. Int. Ed.* **1966,** *5*, 984.
(3) Bonneau, N.; Chen, G.; Lachkar, D.; Boufridi, A.; Gallard, J.-F.; Retailleau, P.; Petek, S.; Debitus, C.; Evanno, L.; Beniddir, M. A.; Poupon, E., *Chem. Eur. J.* **2017,** *23*, 14454.
(4) (a) Braunstein, P.; Siri, O.; Taquet, J.-p.; Yang, Q.-Z., *Angew. Chem. Int. Ed.* **2006,** *45*, 1393; (b) Canard, G.; Chen, Z.; Suryaningtias, A.; Jean, M.; Vanthuyne, N.; Giorgi, M.; Roussel, C.; Siri, O., *New J. Chem.* **2018,** *42*, 8247.
(5) (a) Yang, Q.-Z.; Siri, O.; Braunstein, P., *Chem. Commun.* **2005**, 2660; (b) Tamboura, F. B.; Cazin, C. S. J.; Pattacini, R.; Braunstein, P., *Eur. J. Org. Chem.* **2009,** 3340.
(6) (a) Braunstein, P.; Bubrin, D.; Sarkar, B., *Inorg. Chem.* **2009,** *48*, 2534; (b) Das, H. S.; Das, A. K.; Pattacini, R.; Hübner, R.; Sarkar, B.; Braunstein, P., *Chem. Commun.* **2009**, 4387; (c) Paretzki, A.; Pattacini, R.; Huebner, R.; Braunstein, P.; Sarkar, B., *Chem. Commun.* **2010,** *46*, 1497; (d) Deibel, N.; Hohloch, S.; Sommer, M. G.; Schweinfurth, D.; Ehret, F.; Braunstein, P.; Sarkar, B., *Organometallics* **2013,** *32*, 7366.

(7) (a) Hohloch, S.; Braunstein, P.; Sarkar, B., *Eur. J. Inorg. Chem.* **2012,** 546; (b) Yang, Q.-Z.; Kermagoret, A.; Agostinho, M.; Siri, O.; Braunstein, P., *Organometallics* **2006,** *25*, 5518.
(8) Kar, P.; Yoshida, M.; Shigeta, Y.; Usui, A.; Kobayashi, A.; Minamidate, T.; Matsunaga, N.; Kato, M., *Angew. Chem. Int. Ed.* **2017,** *56*, 2345.
(9) (a) Xiao, J.; Zhang, Z.; Wu, D.; Routaboul, L.; Braunstein, P.; Doudin, B.; Losovyj, Y. B.; Kizilkaya, O.; Rosa, L. G.; Borca, C. N.; Gruverman, A.; Dowben, P. A., *Phys. Chem. Chem. Phys.* **2010,** *12*, 10329; (b) Routaboul, L.; Braunstein, P.; Xiao, J.; Zhang, Z.; Dowben, P. A.; Dalmas, G.; Da Costa, V.; Félix, O.; Decher, G.; Rosa, L. G.; Doudin, B., *J. Am. Chem. Soc.* **2012,** *134*, 8494; (c) Simpson, S.; Kunkel, D. A.; Hooper, J.; Nitz, J.; Dowben, P. A.; Routaboul, L.; Braunstein, P.; Doudin, B.; Enders, A.; Zurek, E., *J. Phys. Chem. C* **2013,** *117*, 16406; (d) Simpson, S.; Hooper, J.; Miller, D. P.; Kunkel, D. A.; Enders, A.; Zurek, E., *J. Phys. Chem. C* **2016,** *120*, 6633; (e) Routaboul, L.; Tanabe, I.; Santana, J. C.; Yuan, M.; Ghisolfi, A.; Garcia, W. S.; Dowben, P. A.; Doudin, B.; Braunstein, P., *RSC Advances* **2017,** *7*, 21906.
(10) (a) Kunkel, D. A.; Simpson, S.; Nitz, J.; Rojas, G. A.; Zurek, E.; Routaboul, L.; Doudin, B.; Braunstein, P.; Dowben, P. A.; Enders, A., *Chem. Commun.* **2012,** *48*, 7143; (b) Koudia, M.; Nardi, E.; Siri, O.; Abel, M., *Nano Res.* **2017,** *10*, 933; (c) Denawi, H.; Koudia, M.; Hayn, R.; Siri, O.; Abel, M., *J. Phys. Chem. C* **2018,** *122*, 15033.
(11) (a) Fang, Y.; Nguyen, P.; Ivasenko, O.; Aviles, M. P.; Kebede, E.; Askari, M. S.; Ottenwaelder, X.; Ziener, U.; Siri, O.; Cuccia, L. A., *Chem. Commun.* **2011,** *47*, 11255; (b) Behyan, S.; Gritzalis, D.; Schmidt, R.; Kebede, E.; Cuccia, L. A.; DeWolf, C., *Phys. Chem. Chem. Phys.* **2019,** *21*, 2345.
(12) Mahmood, A.; Yang, C.-S.; Jang, S.; Routaboul, L.; Chang, H.; Ghisolfi, A.; Braunstein, P.; Bernard, L.; Verduci, T.; Dayen, J.-F.; Samorì, P.; Lee, J.-O.; Doudin, B., *Nanoscale* **2019,** *11*, 19705.
(13) (a) Bailey, A. D.; Murphy, B. P.; Guan, H., *J. Phys. Chem. A* **2016,** *120*, 8512-8520; (b) Zhang, G.; Bailey, A. D.; Bucks, M. E.; Murphy, B. P., *Dyes Pigm.* **2018,** *149*, 167-176.
(14) (a) Hutchison, K.; Srdanov, G.; Hicks, R.; Yu, H.; Wudl, F.; Strassner, T.; Nendel, M.; Houk, K. N., *J. Am. Chem. Soc.* **1998,** *120*, 2989; (b) Wudl, F.; Koutentis, P. A.; Weitz, A.; Ma, B.; Strassner, T.; Houk, K. N.; Khan, S. I., *Pure Appl. Chem.* **1999**; 71, 295; (c) Constantinides, C. P.; Zissimou, G. A.; Berezin, A. A.; Ioannou, T. A.; Manoli, M.; Tsokkou, D.; Theodorou, E.; Hayes, S. C.; Koutentis, P. A., *Org. Lett.* **2015,** *17*, 4026; (d) Zissimou, G. A.; Constantinides, C. P.; Manoli, M.; Pieridou, G. K.; Hayes, S. C.; Koutentis, P. A., *Org. Lett.* **2016,** *18*, 1116; (e) Guevara-Level, P.; Pascal, S.; Siri, O.; Jacquemin, D., *Phys. Chem. Chem. Phys.* **2019,** *21*, 22910.
(15) (a) Pascal, S.; Lavaud, L.; Azarias, C.; Canard, G.; Giorgi, M.; Jacquemin, D.; Siri, O., *Mater. Chem. Front.* **2018,** *2*, 1618; (b) Pascal, S.; Lavaud, L.; Azarias, C.; Varlot, A.; Canard, G.; Giorgi, M.; Jacquemin, D.; Siri, O., *J. Org. Chem.* **2019,** *84*, 1387.
(16) Tang, Q.; Liu, J.; Chan, H. S.; Miao, Q., *Chem. Eur. J.* **2009,** *15*, 3965.
(17) (a) Kolthoff, I. M.; Reddy, T. B., *Inorg. Chem.* **1962,** *1*, 189; (b) Bagno, A.; Scorrano, G., *J. Am. Chem. Soc.* **1988,** *110*, 4577.